J|A|C|S
ARTICLES
Published on Web 02/21/2002

Hydrothermal Oxidation−Reduction Methods for the Preparation of Pure and Single Crystalline Alunites: Synthesis and Characterization of a New Series of Vanadium Jarosites

Daniel Grohol and Daniel G. Nocera*

Contribution from the Department of Chemistry, 6-335, Massachusetts Institute of Technology, 77 Massachusetts Avenue, Cambridge, Massachusetts 02139

Received August 13, 2001

Abstract: Three new redox-based, hydrothermal, synthetic methods have been developed for the preparation of a new series of jarosites, $AV_3(OH)_6(SO_4)_2$ ($A = Na^+$, K^+, Rb^+, Tl^+, and NH_4^+), in high purity and in single crystalline form. The V^{3+} jarosites have been characterized by single-crystal X-ray and elemental analysis, and by infrared and electronic absorption spectroscopy. The synthetic methods employed here represent a new approach for the preparation of the jarosite class of compounds, which for the past several decades, have been notoriously difficult to prepare in pure form. To demonstrate the impact of our new synthetic techniques on the magnetic properties of jarosites, the V^{3+} jarosites were also prepared according to the nonredox techniques used over the past 30 years. A comparative study of these samples and those prepared by our new synthetic methods reveals widely divergent magnetic properties, thus pointing to the importance of the new redox synthetic methods to future magnetism studies of jarosite compounds.

Introduction

The alunite supergroup of minerals consists of more than 40 isostructural compounds with the general formula $AM_3(OH,OH_2)_6(TO_4)_2$.[1] The A site is usually occupied by a monovalent (Na^+, K^+, Rb^+, Tl^+, NH_4^+, H_3O^+), divalent (Ca^{2+}, Ba^{2+}, Pb^{2+}, Hg^{2+}), or a trivalent (Bi^{3+}, rare earths) ion with a coordination number greater or equal to nine, M is occupied by an Al^{3+}, Cr^{3+}, or Fe^{3+} in an octahedral oxygen coordination site, and T is occupied by a S^{6+}, P^{5+}, or As^{5+} in a tetrahedral oxygen site.[1] The three-dimensional structure of the alunites consists of A^+ ions sandwiched between Kagomé layers, which are hexagonal sheets composed of corner-shared triangles of interconnected MO_6 octahedra. These elementary triangles are further capped by TO_4 tetrahedra positioned alternately above and below the two-dimensional layers.[2−7] The placement of spins at the vertices of the triangular array can confer unusual magnetic properties on the Kagomé lattice of exchange-coupled moments.[8] Indeed, the jarosite subgroup of compounds, $AM_3(OH)_6(SO_4)_2$ ($M = Fe^{3+}$ and Cr^{3+}) have long fascinated the solid-state physics community as models for studying the phenomenon called spin-frustration arising from antiferromagnetic coupling of spins about the triangular lattice.[9−22] When the spins are ferromagnetically coupled, as has been recently found for the Na^+ form of V^{3+} jarosite,[23,24] metamagnetism of the pseudo-XY type is observed.[25]

Despite nearly three decades of intense research, the magnetism of the jarosite compounds continues to elude complete characterization. In such highly correlated systems, very pure and stoichiometric samples are required to obtain consistent and

(1) Jambor, J. L. *Can. Mineral.* **1999**, *37*, 1323−1341.
(2) Szymañski, J. T. *Can. Mineral.* **1985**, *23*, 659−668.
(3) Kato, T.; Miura, Y. *Mineral. Mag.* **1977**, *8*, 419−430.
(4) Menchetti, S.; Sabelli, C. *Neues Jahrb. Mineral. Monatsh.* **1976**, 406−417.
(5) Takano, M.; Shinjo, T.; Takada, T. *J. Phys. Soc. Jpn.* **1971**, *30*, 1049−1053.
(6) Wang, R.; Bradley, W. F.; Steinfink, H. *Acta Crystallogr.* **1965**, *18*, 249−252.
(7) Hendricks, S. B. *Am. Mineral.* **1937**, *22*, 773−784.
(8) Ramirez, A. P. *Annu. Rev. Mater. Sci.* **1994**, *24*, 453−480.
(9) Wills, A. S.; Harrison, A. *J. Chem. Soc., Faraday Trans.* **1996**, *92*, 2161−2166.
(10) Wills, A. S.; Harrison, A.; Ritter, C.; Smith, R. I. *Phys. Rev. B* **2000**, *61*, 6156−6169.
(11) Inami, T.; Nishiyama, M.; Maegawa, S.; Oka, Y. *Phys. Rev. B* **2000**, *61*, 12181−12186.
(12) Frunzke, J.; Hansen, T.; Harrison, A.; Lord, J. S.; Oakley, G. S.; Visser, D.; Wills, A. S. *J. Mater. Chem.* **2001**, *11*, 179−185.
(13) Earle, S. A.; Ramirez, A. P.; Cava, R. J. *Physica B* **1999**, *262*, 199−204.
(14) Harrison, A.; Wills, A. S.; Ritter, C. *Physica B* **1998**, *241−243*, 722−723.
(15) Oakley, G. S.; Pouget, S.; Harrison, A.; Frunzke, J.; Visser, D. *Physica B* **1999**, *267−268*, 145−148.
(16) Oakley, G. S.; Visser, D.; Frunzke, J.; Andersen, K. H.; Wills, A. S.; Harrison, A. *Physica B* **1999**, *267−268*, 142−144.
(17) Wills, A. S.; Harrison, A.; Mentink, S. A. M.; Mason, T. E.; Tun, Z. *Europhys. Lett.* **1998**, *42*, 325−330.
(18) Keren, A.; Kojima, K.; Le, L. P.; Luke, G. M.; Wu, W. D.; Uemura, Y. J.; Takano, M.; Dabkowska, H.; Gingras, M. J. P. *Phys. Rev. B* **1996**, *53*, 6451−6454.
(19) Maegawa, S.; Nishiyama, M.; Tanaka, N.; Oyamada, A.; Takano, M. *J. Phys. Soc. Jpn.* **1996**, *65*, 2776−2778.
(20) Townsend, M. G.; Longworth, G.; Roudaut, E. *Phys. Rev. B* **1986**, *33*, 4919−4926.
(21) Reimers, J. N.; Berlinsky, A. J. *Phys. Rev. B* **1993**, *48*, 9539−9554.
(22) Lee, S.-H.; Broholm, C.; Collins, M. F.; Heller, L.; Ramirez, A. P.; Kloc, Ch.; Bucher, E.; Erwin, R. W.; Lacevic, N. *Phys. Rev. B* **1997**, *56*, 8091−8097.
(23) Grohol, D.; Papoutsakis, D.; Nocera, D. G. *Angew. Chem., Int. Ed.* **2001**, *40*, 1519−1521.
(24) Papoutsakis, D.; Grohol, D.; Nocera, D. G. *J. Am. Chem. Soc.* **2002**, *124*, 2647−2656.
(25) Grohol, D.; Huang, Q. Z.; Lee, Y. S.; Toby, B. H.; Lynn, J. W.; Nocera, D. G. Manuscript in preparation.

10.1021/ja016832u CCC: $22.00

reproducible results. Whereas synthetic approaches to the jarosites have been studied extensively in conjunction with their utility in the zinc refinery industry,[26,27] methods have relied exclusively on the simple precipitation at 100−160 °C of jarosite from aqueous solutions containing the constituent ions A^+, M^{3+}, and SO_4^{2-} ions,[28−30]

$$A^+ + 3M^{3+} + 2SO_4^{2-} + 6H_2O \rightarrow AM_3(OH)_6(SO_4)_2 + 6H^+ \quad (1)$$

Precipitation of jarosites under these conditions occurs quickly to yield small crystallites of 5−20 μm. Moreover, the maximum occupancy of magnetic sites has been observed to be only 97%, with most methods providing samples possessing magnetic site occupancies of 83−94%.[9] Accordingly, the low and varying coverage of the M^{3+} sites in jarosite materials have led to considerable discrepancies in their reported magnetic properties.

With the objective of using the jarosite structural framework as a model system for investigating the magnetic properties of the Kagomé lattice, we sought to develop new synthetic methods for the preparation of pure and highly crystalline materials. Our synthetic approaches rely on employing redox-based hydrothermal methods to control the kinetics of product precipitation. Here we report the development of such methods for the synthesis and physical characterization of a new series of magnetically pure and highly crystalline V^{3+} jarosites, $AV_3(OH)_6(SO_4)_2$ with A = Na^+, K^+, Rb^+, Tl^+, and NH_4^+. As discussed in the following paper,[24] this class of compounds allows for the systematic investigation of the magnetic properties of a material composed of ferromagnetic Kagomé layers at varying distances of separation.

Experimental Section

General Procedures. All chemicals of reagent or analytical grade were obtained from commercial companies, and they were used without purification. Hydrothermal reactions were carried out in 23-mL, 45-mL and 125-mL Teflon-lined, pressure vessels, which were purchased from Parr Instruments. A Fisher Isotemp programmable oven with forced-air circulation was used to obtain the desired temperature profiles for hydrothermal reactions.

Synthesis by Hydrothermal Redox Methods: Preparation of $NaV_3(OH)_6(SO_4)_2$ (NaVS). Method 1. VCl_4 (5.3 mL) was added dropwise to a stirring solution of ∼10 mL of ice-cold water; the resulting reaction mixture was diluted to 25 mL to afford a solution that was 2.0 M in $VOCl_2$ and 4.0 M in HCl. A 2.0-mL amount of this solution (4.0 mmol of $VOCl_2$) was transferred into the Teflon liner of a 23-mL pressure vessel. In a separate beaker, 0.227 g (1.80 mmol) of Na_2SO_3, 0.20 g (5.0 mmol) of NaOH and 0.117 g (2.0 mmol) of NaCl were dissolved in 8 mL of distilled water, and the solution was slowly added to the $VOCl_2$-charged Teflon liner. The vessel was sealed and placed into an oven at 202 °C. After 6 d, the oven was cooled at 0.1 °C min^{-1} to room temperature. Small, dark-red to black crystals were filtered, washed with distilled water, and dried in air. Yield: 0.31 g (73%). Anal. Calcd for $H_6NaV_3S_2O_{14}$: H 1.29, Na 4.89, V 32.52, S 13.65. Found: H 1.32, Na 5.06, V 32.85, S 13.88.

Method 2. Ten milliliters of a 2.0 M $VOCl_2$ solution (20 mmol), prepared as described above, was mixed with a 50-mL solution containing 1.00 g (25 mmol) of NaOH in a 125-mL Teflon liner. To this solution, 0.86 mL (10 mmol) of dimethylsulfite was added. The pressure vessel was closed and placed into an oven at 202 °C for 6 d. The oven was then cooled at 0.1 °C min^{-1} to room temperature. Small, dark-red crystals were filtered, washed, and dried in air. Yield: 1.22 g (52%). Anal. Calcd for $H_6NaV_3S_2O_{14}$: H 1.29, Na 4.89, V 32.52, S 13.65. Found: H 1.33, Na 4.95, V 32.42, S 13.46.

Method 3. To 2.84 g of Na_2SO_4 (20.0 mmol) dissolved in 50 mL of distilled water was added 1.94 mL (35 mmol) of H_2SO_4. The solution was transferred into a Teflon liner of a 125-mL pressure vessel. A 0.51-g pellet of metallic vanadium (10 mmol) was added to this solution. The enclosed vessel was placed into an oven at 200 °C for 4 d. The oven was then cooled at 0.1 °C min^{-1} to room temperature. After opening the vessel, a small, unreacted piece of vanadium metal covered with V^{3+} jarosite was carefully removed. The product that precipitated on the walls of the Teflon liner was isolated, washed with distilled water and dried in air. Yield: 0.91 g (58%). Anal. Calcd for $H_6NaV_3S_2O_{14}$: H 1.29, Na 4.89, V 32.52, S 13.65. Found: H 1.32, Na 4.95, V 32.61, S 13.74.

Preparation of $KV_3(OH)_6(SO_4)_2$ (KVS). Method 1. A 45-mL Parr pressure vessel was charged with 4.0 mL of 2.0 M $VOCl_2$ (8.0 mmol). In a separate beaker, 0.316 g of K_2SO_3 (2.0 mmol), and 0.112 g of KOH (2.0 mmol) was dissolved in 16 mL of distilled water and slowly added to the Teflon liner containing the $VOCl_2$ solution. The vessel was sealed and placed into an oven at 205 °C for 4 d. The oven was then cooled at 0.1 °C min^{-1} to room temperature. The product precipitated on the walls of the Teflon liner; it was isolated, washed with distilled water, and dried in air. Yield: 0.27 g (58%). Anal. Calcd for $H_6KV_3S_2O_{14}$: H 1.24, K 8.04, V 31.44, S 13.19. Found: H 1.25, K 8.11, V 31.38, S 13.32.

Method 2. A 2.0-mL amount of a 2.0 M $VOCl_2$ solution (4.0 mmol) was mixed with 10 mL of solution containing 0.22 g (4.0 mmol) of KOH in a 23-mL Teflon liner. Into this solution, 0.18 mL (2.1 mmol) of dimethylsulfite was added, and the Parr vessel was sealed. The enclosed solution was heated at 202 °C for 7 d after which the oven was cooled at 0.1 °C min^{-1} to room temperature. Small, dark-red crystals that attached to the walls of the Teflon liner were collected by filtration, washed with distilled water, and dried in air. Yield: 0.21 g (41%). Anal. Calcd for $H_6KV_3S_2O_{14}$: H 1.24, K 8.04, V 31.44, S 13.19. Found: H 1.26, K 8.04, V 31.36, S 13.25.

Method 3. To a solution of 4.36 g of K_2SO_4 (25 mmol) dissolved in 50 mL of distilled water was added 1.94 mL (35 mmol) of H_2SO_4; the resulting solution was transferred into a Teflon liner of a 125-mL pressure vessel. A 0.538-g pellet of metallic vanadium (10.5 mmol) was added to the solution, the vessel was enclosed and placed into an oven at 205 °C for 7 d. The oven was then cooled at 0.1 °C min^{-1} to room temperature. After opening the vessel, a small, unreacted piece of vanadium metal was carefully removed. The product that precipitated on the walls and on the bottom was isolated, washed with distilled water, and dried in air. Yield: 0.58 g (34%). Anal. Calcd for $H_6KV_3S_2O_{14}$: H 1.24, K 8.04, V 31.44, S 13.19. Found: H 1.20, K 7.96, V 31.19, S 13.11.

Preparation of $RbV_3(OH)_6(SO_4)_2$ (RbVS). Method 1. A 2.0-mL aliquot of a 2.0 M $VOCl_2$ solution (4.0 mmol) was transferred into a Teflon liner of a 23-mL Parr pressure vessel. In a separate beaker, 0.47 mL of a 50% solution of RbOH (4.0 mmol) and 2.1 mL of 6% H_2SO_3 (2.0 mmol) were dissolved in 6 mL of distilled water and slowly added to the Teflon liner containing $VOCl_2$. The bomb was sealed and placed into an oven at 205 °C for 4 d. The oven was then cooled at 0.1 °C min^{-1} to room temperature. The product that precipitated on the walls of the Teflon liner was isolated, washed with distilled water, and dried in air. Yield: 0.18 g (34%). Anal. Calcd for $H_6RbV_3S_2O_{14}$: H 1.14, Rb 16.05, V 28.70, S 12.04. Found: H 1.12, Rb 15.57, V 31.12, S 12.03.

Method 2. A 2.0-mL amount of 2.0 M $VOCl_2$ solution was mixed with 8 mL of solution containing 0.59 mL (5.0 mmol) of 50% RbOH in a 23-mL Teflon liner. Into this solution, 0.18 mL (2 mmol) of

(26) Buban, K. R.; Collins, M. J.; Masters, I. M. *JOM* **1999**, *51*, 23−25.
(27) Dutrizac, J. E. *JOM* **1999**, *51*, 30−32.
(28) Dutrizac, J. E. *Metall. Trans. B* **1983**, *14*, 531−539.
(29) Dutrizac, J. E.; Kaiman, S. *Can. Mineral.* **1976**, *14*, 151−158.
(30) Kubisz, J. *Mineral. Polonica* **1970**, *1*, 47−57.

dimethylsulfite was added. The bomb was closed and placed into the oven at 202 °C for 7 d. The oven was then cooled at 0.1 °C min^{-1} to room temperature. Small dark-red crystals attached to the walls of the Teflon liner were filtered, washed, and dried in air. Yield: 0.35 g (66%). Anal. Calcd for $H_6RbV_3S_2O_{14}$: H 1.14, Rb 16.05, V 28.70, S 12.04. Found: H 1.10, Rb 16.12, V 29.11, S 12.07.

Method 3. To a solution of 3.74 g of Rb_2SO_4 (14 mmol) dissolved in 50 mL of distilled water was added 1.94 mL (35 mmol) of H_2SO_4, and the solution was transferred into a Teflon liner of a 125-mL pressure vessel. A 0.616-g pellet of metallic vanadium (12.1 mmol) was added to the solution. The vessel was enclosed and placed into an oven at 204 °C for 7 d. The oven was cooled at 0.1 °C min^{-1} to room temperature, and after opening the vessel, a small, unreacted piece of vanadium metal was carefully removed. The product that precipitated on the walls and on the bottom of the liner was isolated, washed with distilled water, and dried in air. Yield: 1.14 g (53%). Anal. Calcd for $H_6RbV_3S_2O_{14}$: H 1.14, Rb 16.05, V 28.70, S 12.04. Found: H 1.06, Rb 16.28, V 28.88, S 12.10.

Preparation of $TlV_3(OH)_6(SO_4)_2$ (TlVS). Method 1. A solution of 1.01 g of Tl_2SO_4 (2.0 mmol) dissolved in 5.5 mL of distilled water and 3.1 mL (3.0 mmol) of 0.96 M H_2SO_3 was transferred into a Teflon liner of a 23-mL Parr pressure vessel containing 1.5 mL of 2.0 M $VOCl_2$ (3.0 mmol). The vessel was sealed and placed into an oven at 205 °C for 3 d. The oven was then cooled at 0.1 °C min^{-1} to room temperature. The product was isolated, washed with distilled water, and dried in air. This method produced a heterogeneous mixture of dark maroon crystals of TlVS and colorless crystals of TlCl. Crystals from this synthetic procedure were of high quality and were characterized structurally by single-crystal analysis. The TlVS jarosite could not be obtained in the absence of TlCl due to this salt's very low solubility in water. To obtain TlCl-free TlVS, the following procedure was developed to permit the separation of the two phases. A 2.0-mL amount of 2.0 M $VOCl_2$ was added into a Teflon liner of a 23-mL Parr pressure vessel, and 2 mL of distilled water was added. In a separate beaker, 0.938 g of Tl_2CO_3 was added to 6.16 mL of 0.65 M solution of H_2SO_3 (4.0 mmol), and the mixture was added to the Teflon liner. The bomb was enclosed and placed into an oven at 205 °C for 5 d. The oven was then cooled at 0.1 °C min^{-1} to room temperature. White precipitate of TlCl covered the bottom of the liner while dark maroon precipitate of product formed on the walls. The product was collected. Yield: 0.13 g (20%). Anal. Calcd for $H_6TlV_3S_2O_{14}$: H 0.93, Tl 31.38, V 23.46, S 9.85. Found: H 1.04, Tl 32.37, V 23.62, S 9.87.

Method 2. A 23-mL Teflon-lined Parr vessel containing 0.938 g (2.0 mmol) of Tl_2CO_3, 0.18 mL of dimethylsulfite (2.0 mmol), 2.0 mL of 2.0 M $VOCl_2$ (4.0 mmol), and 8 mL of distilled water was sealed and placed in an oven at 202 °C for 3 d. The oven was then cooled at 0.1 °C min^{-1} to room temperature. A white precipitate of TlCl covered the bottom of the liner, and maroon TlVS precipitated on the walls. Yield: 0.093 g (14%). Anal. Calcd for $H_6TlV_3S_2O_{14}$: H 0.93, Tl 31.38, V 23.46, S 9.85. Found: H 1.06, Tl 32.18, V 23.58, S 9.79.

Method 3. In 9.6 mL of distilled water were dissolved 0.151 g of Tl_2SO_4 (0.30 mmol) and 0.44 mL of H_2SO_4, and the solution was transferred into a Teflon liner of a 23-mL pressure bomb. A 0.163-g pellet of metallic vanadium (3.2 mmol) was added to the solution, and the bomb was enclosed and placed into an oven at 205 °C for 4 d. The oven was then cooled at 0.6 °C min^{-1} to room temperature. After opening the bomb, a small, unreacted piece of vanadium metal was removed. The product that precipitated on the walls and on the bottom was carefully isolated, washed with distilled water, and dried in air. Yield: 0.130 g (33%). Anal. Calcd for $H_6TlV_3S_2O_{14}$: H 0.93, Tl 31.38, V 23.46, S 9.85. Found: H 0.75, Tl 31.43, V 23.80, S 10.08.

Preparation of $NH_4V_3(OH)_6(SO_4)_2$ (NH_4VS). Method 1. A 2.0-mL amount of 2.0 M $VOCl_2$ solution (4.0 mmol) was transferred into a Teflon liner of a 23-mL Parr pressure bomb. In a separate beaker, 0.54 mL of a 14.8 M solution of NH_4OH (8.0 mmol), and 2.1 mL of 6% H_2SO_3 (2.0 mmol) were dissolved in 6.0 mL of distilled water, and the resulting solution was slowly added to the bomb, which was then closed and placed into an oven at 200 °C for 3 d. The bomb was cooled to room temperature at 0.1 °C min^{-1}. The product, which precipitated on the walls of the liner, was isolated, washed with distilled water, and dried in air. Yield: 0.22 g (47%). Anal. Calcd for $H_{10}NV_3S_2O_{14}$: H 2.17, N 3.01, V 32.86, S 13.79. Found: H 2.14, N 2.93, V 32.74, S 13.65.

Preparation by Conventional Non-Redox Methods: Preparation of NaVS. A 25-mL round-bottom flask was charged with a 10-mL aqueous solution containing 1.420 g of Na_2SO_4 (10 mmol) and 0.040 g of NaOH (1.0 mmol). After the addition of 0.551 g of VCl_3 (3.5 mmol), the flask was fitted with a condenser, and the solution was refluxed for 24 h. The resulting suspension was cooled to room temperature. A green precipitate was collected by filtration, washed with distilled water, and air-dried. Yield: 0.49 g (84%). Analysis revealed that the occupancy of the magnetic sites was 91.7% and that 25% of the Na^+ sites were substituted by the H_3O^+ ions. Anal. Calcd for $H_{7.5}Na_{0.75}V_{2.75}S_2O_{14.25}$: H 1.64, Na 3.78, V 30.66, S 14.01. Found: H 2.16, Na 3.85, V 30.48, S 13.43.

Crystallography. X-ray diffraction data were collected using a Siemens three-circle single-crystal diffractometer equipped with a CCD detector. All the data acquisitions were carried out at −90 °C in a nitrogen stream using Mo Kα radiation ($\lambda = 0.71073$ Å), which was wavelength-selected with a single-crystal graphite monochromator. For each crystal, four data sets of 40-s frames were collected over a hemisphere of reciprocal space using ω scans and a −0.3° scan width. The data frames were integrated to *hkl*/intensity, and final unit cells were calculated using the SAINT program. All structures were solved by the Patterson methods and refined using the SHELXTL suite of programs.

Methods. Electronic absorption spectra were measured on an OLIS-modified Cary-17 spectrophotometer. Solid samples of V^{3+} jarosites were finely ground, suspended in Nujol mull, and spread on Whatman 1 filter paper. All spectra were recorded over a spectral range of 360−800 nm against a reference consisting of another filter paper moistened with several drops of Nujol.

Infrared spectra of jarosites in KBr pellets were recorded on a Nicolet Magna-IR 860 Spectrometer equipped with a KBr beam splitter and a DTGS detector. For each spectrum, 32 scans were acquired with 4-cm^{-1} resolution over a wavelength range of 4000−400 cm^{-1}.

Magnetic susceptibilities of powdered samples prepared by conventional nonredox method were measured in gelatin capsules using a SQUID susceptometer (Quantum Design MPMSR2) over a 6−300 K temperature range and at 0.5, 5.0, and 10.0 kOe. The Curie−Weiss constants were calculated from linear fits of the inverse susceptibilities vs temperature for $T = 150-300$ K.

Results and Discussion

Syntheses. Five analogues of vanadium jarosite $AV_3(OH)_6(SO_4)_2$ (A = Na^+, K^+, Rb^+, Tl^+ and NH_4^+) have been prepared by three different hydrothermal, redox-based methods. With each of the synthetic approaches, we have achieved control over the precipitation of the jarosite by using redox reactions to slowly generate V^{3+} throughout the course of the hydrothermal process. Each of the approaches yields single-crystalline and highly pure samples that analyze as 100.3 ± 1.1% in the M^{3+} ion, 100 ± 1.5% in the A^+ ion, 99.5 ± 1.1% in S, and 99.5 ± 3% in H. Given the large standard deviation of the latter value, we note that the elemental analysis does not reliably establish the hydrogen content. In principle, missing protons from the lattice could be charge-compensated by the presence of vanadium ions in a +4 oxidation state. Our neutron diffractions studies, however, have established that fully reduced V^{3+} materials are obtained from the redox-based synthetic methods described

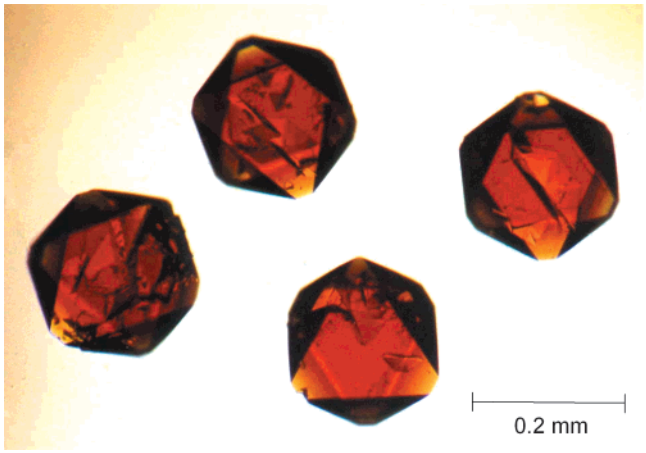

Figure 1. Photograph of single crystals of $KV_3(OH)_6(SO_4)_2$ prepared by method 3.

here.[25] Figure 1 shows typical crystals, which are trigonal antiprismatic plates of approximate dimensions of 0.2 mm × 0.2 mm in width and 0.04 mm in thickness. The orange crystals darken in intensity with increasing crystal size.

The V^{3+} ion may be prepared by reducing V^{4+} in the form of $VOCl_2$ by sulfite anion SO_3^{2-} in the presence of the A^+ cations under acidic conditions (pH ≈ 1.5),

$$A^+ + 4\,VO^{2+} + 2\,SO_3^{2-} + 4\,H_2O \rightarrow AV_3(OH)_6(SO_4)_2 + V^{3+} + 2\,H^+ \quad (2)$$

The main constituent building blocks of the jarosite lattice, the V^{3+} and SO_4^{2-} ions, are produced by a redox reaction. During the course of the overall reaction, the pH of the reaction mixture increases, attendant to the incorporation of hydroxides into the V^{3+} jarosite lattice; two moles of protons are generated per mole of $AV_3(OH)_6(SO_4)_2$ produced. Small crystals are obtained from reaction 2.

Dimethylsulfite, $(CH_3O)_2SO$, is also a competent reductant of $VOCl_2$ under hydrothermal conditions at 200 °C,

$$A^+ + 4\,VO^{2+} + 2\,(CH_3O)_2SO + 8\,H_2O \rightarrow AV_3(OH)_6(SO_4)_2 + V^{3+} + 6\,H^+ + 4\,CH_3OH \quad (3)$$

This method leads to pure jarosites of high crystal quality, but the size of the crystals is not significantly improved with respect to the approach based on reaction 2.

Alternatively, V^{3+} may be produced by oxidation of V metal. Under hydrothermal conditions, oxygen or protons present in the reacting solution are the potential oxidants. To distinguish between these possibilities, two reactions were performed under identical hydrothermal conditions with the exception that one was performed under an oxygen atmosphere and the other under a nitrogen atmosphere. In both cases, V^{3+} jarosite was obtained with similar yields. This result indicates that oxygen is not essential for the formation of V^{3+} and consequently that protons are the primary oxidant of V metal,

$$V + 3\,H^+ \rightarrow V^{3+} + {}^3/_2\,H_2 \quad (4)$$

With the coupling of reaction 4 to 1, this hydrothermal method consumes three equiv of protons per equiv of V^{3+} jarosite produced. Unlike methods 1 and 2, the acidity of the solution decreases slowly during this reaction. The oxidation method most often yields samples of the highest-quality single crystals. We believe that the dissolution of metallic vanadium provides a means of slowly generating V^{3+} ion, which is likely the controlling step of the crystallization process. The preparative method does, however, present one inconvenience. The reaction does not proceed to completion due to passivation of the vanadium pellet, which must be physically removed from the vessel prior to collecting the jarosite product.

Structural Chemistry. The layered Kagomé motif of the alunite supergroup of compounds of formula $AM_3(OH)_6(SO_4)_2$ was first established by X-ray single-crystal analysis of a natural potassium alunite sample.[7] The correct space group for the alunites was subsequently determined to be $R\bar{3}m$.[6] The structures of the new V^{3+} jarosites reported here conform to this latter result, all crystallizing in the $R\bar{3}m$ space group. Crystallographic data of the Na^+, K^+, Rb^+, and Tl^+ derivatives are reported in Table 1, and selected bond distances and angles, in Table 2. Crystals of the NH_4^+ derivative were not of sufficient quality to permit single-crystal data to be acquired. Consistent with the initial structural reports of NaVS,[23,31] the triangular subunit of the Kagomé lattice is composed of a sulfate anion, which caps three vanadium octahedra that form a layered corner-sharing triangular network (Figure 2a). This basic building block is not perturbed by the A^+ ion. A comparison of the derivatives reveals that the *a*-dimension of the unit cell (Figure 2b) and all equivalent bond distances and angles within the basic layer framework are almost identical (Table 2). The only structural value that appreciably changes within the series is the *c*-dimension of the unit cell (Figure 2c), which is dictated by the size of the monovalent cation residing between the Kagomé layers. The monotonic increase in the interlayer spacing along the series NaVS (d_{003} = 5.617 Å), KVS (d_{003} = 5.800 Å), RbVS (d_{003} = 5.945 Å), and TlVS (d_{003} = 5.800 Å) follows directly from the increasing ionic radius of the monocation.

Spectroscopic and Magnetic Characterization. Electronic absorption spectra of the Na^+, K^+, and Rb^+ derivatives are almost identical. The visible absorption spectrum shows two distinct shoulders at 410 and 570 nm. The energies of these absorption bands are similar to those observed for the ${}^3T_{1g}(P) \leftarrow {}^3T_{1g}$ (λ_{max} = 389 nm) and ${}^3T_{2g} \leftarrow {}^3T_{1g}$ (λ_{max} = 561 nm) transitions of $V(H_2O)_6^{3+}$, respectively.[32] An oxide ligand field even more closely approximates that of the V^{3+} jarosites. The observed transitions of V^{3+} doped into the pseudooctahedral oxide environment provided by Al_2O_3 appear at 401 and 574 nm.[32]

Infrared spectra of the Na^+, K^+, and Rb^+ derivatives are very similar to each other. The spectrum of the Na^+ derivative shown in Figure 3 is exemplary of the series. A very strong peak with a maximum between 3420 and 3360 cm^{-1} and an equally strong peak at 1030 cm^{-1} are attributed to the absorptions of the O(3)−H stretching and V−O(3)−H bending modes, respectively.[33−35] The energy of the O−H stretching mode increases along the series NaVS < KVS < RbVS by 25 and 27 cm^{-1}, respectively (Table 3), suggesting the relative strength of the A^+−O interaction to follow the trend: Na^+−O(3) > K^+−O(3)

(31) Dobley, A.; Zavalij, P. Y.; Whittingham, M. S. *Acta Crystallogr. C* **2000**, *56*, 1294−1295.
(32) Lever, A. B. P. *Inorganic Electronic Spectroscopy*; Elsevier: Amsterdam, 1984; Chapter 6, pp 400−405.

Table 1. Crystallographic Data for the $AV_3(OH)_6(SO_4)_2$ Jarosites

	NaVS	KVS	RbVS	TlVS
empirical formula	$H_6NaV_3S_2O_{14}$	$H_6KV_3S_2O_{14}$	$H_6RbV_3S_2O_{14}$	$H_6TlV_3S_2O_{14}$
fw	469.99	486.09	532.46	651.38
crystal system	rhombohedral	rhombohedral	rhombohedral	rhombohedral
space group	$R\bar{3}m$	$R\bar{3}m$	$R\bar{3}m$	$R\bar{3}m$
a (Å)	7.2857(6)	7.2737(7)	7.281(2)	7.2834(6)
c (Å)	16.851(2)	17.399(2)	17.835(7)	17.919(2)
α (deg)	90	90	90	90
γ (deg)	120	120	120	120
Z; V (Å^3)	3; 774.6(1)	3; 797.2(2)	3; 818.8(5)	3; 823.2(2)
ρ_{calc}	3.022	3.037	3.239	3.941
θ range (deg)	3.45−23.25	3.44−23.09	3.43−23.27	3.41−23.26
scan	ω	ω	ω	ω
temp (K)	183(2)	183(2)	183(2)	183(2)
no. of reflections collected	1050	1048	1087	1137
no. of unique reflections	161	160	172	173
no. of parameters	25	25	25	25
R1 ($I > 2\sigma$; all data)	0.0295; 0.0306	0.0400; 0.0407	0.0365; 0.0412	0.0210; 0.0218
wR2 ($I > 2\sigma$; all data)	0.0789; 0.0792	0.0973; 0.0975	0.0918; 0.0935	0.0474; 0.0479
GOF	1.318	1.288	1.240	1.263

Table 2. Selected Bond Distances (Å) and Bond Angles (deg) for the $AV_3(OH)_6(SO_4)_2$ Jarosites

	NaVS	KVS	RbVS	TlVS
	Bond Distances/Å			
A−O(2) 6×	2.949(5)	2.975(6)	2.998(6)	3.002(6)
A−O(3) 6×	2.756(4)	2.851(5)	2.928(6)	2.943(5)
S−O(1)	1.461(8)	1.46(1)	1.46(1)	1.47(1)
S−O(2) 3×	1.476(5)	1.471(6)	1.478(7)	1.486(6)
V−O(2) 2×	2.054(4)	2.063(5)	2.064(6)	2.055(5)
V−O(3) 4×	1.989 (2)	1.991(2)	1.988(3)	1.983(2)
	Bond Angles/deg			
O(1)−S−O(2) 3×	109.4(2)	109.7(2)	110.0(3)	110.2(2)
O(2)−S−O(2) 3×	109.6(2)	109.2(2)	109.0(3)	108.8(2)
O(2)−V−O(2)	180	180	180	180
O(2)−V−O(3) 4×	92.5 (1)	92.4 (2)	92.0(2)	91.6 (2)
O(2)−V−O(3) 4×	87.5(1)	87.6 (2)	88.0(2)	88.4(2)
O(3)−V−O(3) 2×	180	180	180	180
O(3)−V−O(3) 2×	90.9(3)	90.5(3)	91.0(4)	90.5(3)
O(3)−V−O(3) 2×	89.1(3)	89.5(3)	89.0(4)	89.5(3)

> Rb^+−O(3). Two very strong peaks at about 1190 and 1095 cm^{-1} arise from the antisymmetric S−O stretching modes of the sulfate anion, and two medium peaks at 702 and 642 cm^{-1} are due to the S−O bending modes of the same moiety. A very strong peak at 521 cm^{-1} is indicative of the V−O stretching mode.

Two prominent IR absorption features distinguish V^{3+} jarosites prepared by the new redox-based methods from those materials obtained with the conventional precipitation methods employed previously to this study. As shown by the dashed line of Figure 3, the IR spectrum of V^{3+} jarosite prepared by nonredox methods exhibits a broad absorption near 3400 cm^{-1} for the O−H stretching vibration and an absorption at 1635 cm^{-1}, which is characteristic of an H−O−H bending mode. In stoichiometrically pure jarosites, the 3400 cm^{-1} absorption is reduced in intensity and width; the 1635 cm^{-1} does not appear because the H−O−H moiety is not intrinsic to the jarosite structure. We believe that this result indicates a significant presence of two extrinsic species in jarosites prepared by conventional methods. One is the H_3O^+ ion, which can substitute for the interlayer A^+ cation,

$$AM_3(OH)_6(SO_4)_2 + x\ H_3O^+ \rightarrow A_{1-x}(H_3O)_xM_3(OH)_6(SO_4)_2 \quad (5)$$

The other species is H_2O resulting from the protonation of the intralayer hydroxy group. For jarosites with M^{3+} ion deficiencies, proton transfer permits the charge neutrality of the compound to be maintained.

$$AV_3(OH)_6(SO_4)_2 + 3x\ H^+ \rightarrow AV_{3-x}(OH_2)_{3x}(OH)_{6-3x}(SO_4)_2 \quad (6)$$

Our contention of extrinsic impurities consisting of H_2O and H_3O^+ is confirmed by the elemental analysis of the NaVS sample prepared by the conventional nonredox technique; an analysis of $Na_{0.75}(H_3O)_{0.25}V_{2.75}(OH_2)_{0.75}(OH)_{5.25}(SO_4)_2$ indicates the presence of significant deficiencies in the contents of both the Na^+ and the V^{3+} ions. Therefore, both types of defects are present in the lattice. The presence of both inter- and intralayer defects have significant implications for the magnetic properties, particularly for the nature of long-range ordering (vide infra).

Jarosite materials prepared by redox and nonredox hydrothermal methods exhibit profoundly different magnetic properties. Plots of χ_M^{-1} vs T for $T = 150-300$ K are linear for all samples. For the sodium member of the series, similar Curie−Weiss constants of $\Theta_{CW} = 53(2)$ K and 50(2) K are obtained for samples prepared by redox- and nonredox methods, respectively. However, the magnetic properties of samples prepared by the different methods are not commensurate in the low-temperature region ($T < 40$ K). Figure 4 emphasizes the magnetic susceptibility plots of NaVS over the low-temperature range where three-dimensional antiferromagnetic ordering between neighboring Kagomé layers becomes evident.[23,24] The critical ordering temperature, $T_c = 20.5$ K, of the sample prepared by the conventional precipitation technique is significantly lower than the $T_c = 33.3$ K observed for samples prepared by the new redox technique. A similar result is observed for the KVS samples (T_c (0.5 kOe) = 15.5 K and T_c (0.5 kOe) = 31.0 K for nonredox and redox prepared samples, respectively). These results indicate that the nature of the long-range interactions is significantly influenced by lattice defects associated with

(33) Powers, D. A.; Rossman, G. R.; Schugar, H. J.; Gray, H. B. *J. Solid State Chem.* **1975**, *13*, 1−13.
(34) Ripmeester, J. A.; Ratcliffe, C. I.; Dutrizac, J. E.; Jambor, J. L. *Can. Mineral.* **1986**, *24*, 435-447 and references therein.
(35) Sasaki, K.; Tanaike, O.; Konno, H. *Can. Mineral.* **1998**, *36*, 1225−1235.

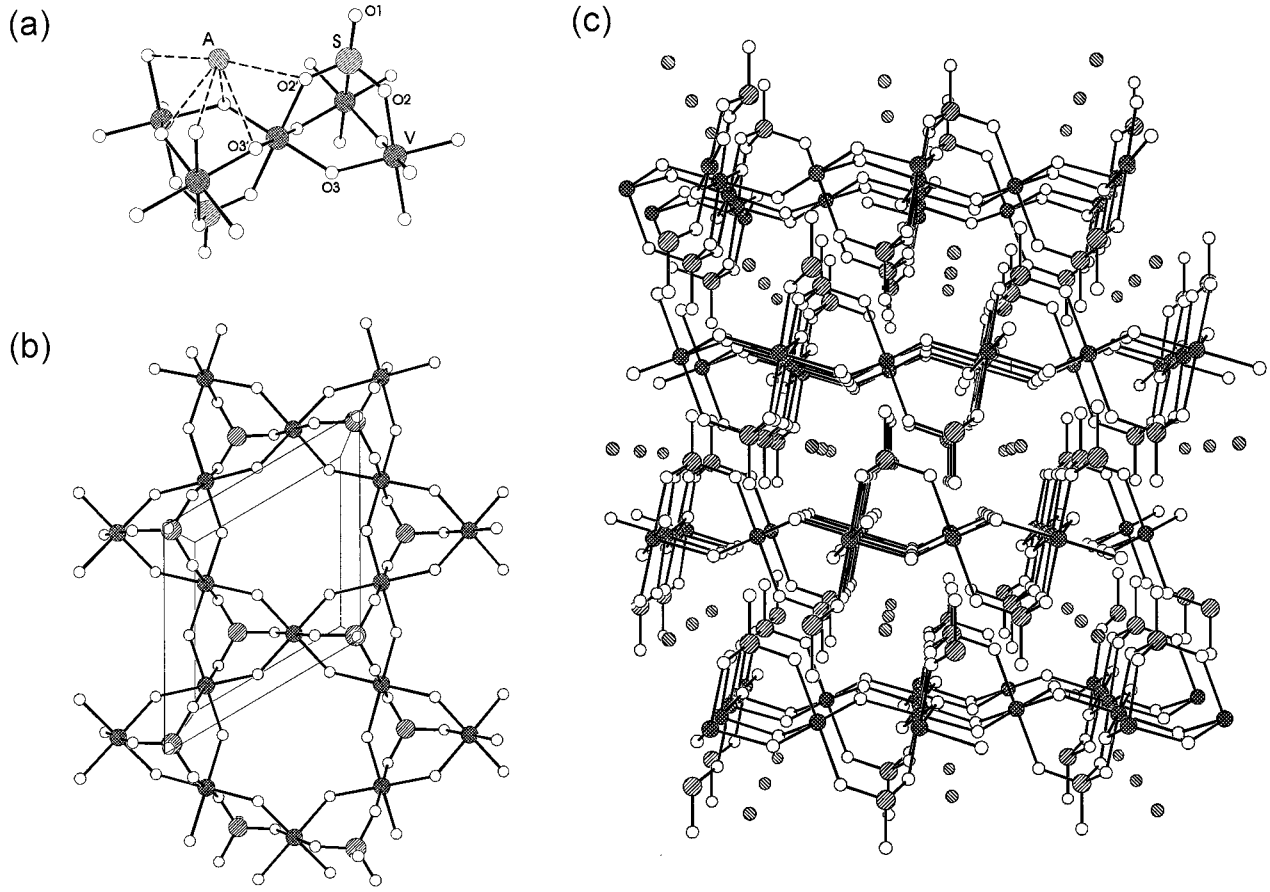

Figure 2. The X-ray crystal structure of (a) the magnetic subunit of a triangular μ-hydroxy vanadium trimer, (b) the in-plane segment of the Kagomé layer and (c) side-on view of stacked Kagomé layers. The sphere coding of the atoms is presented in (a).

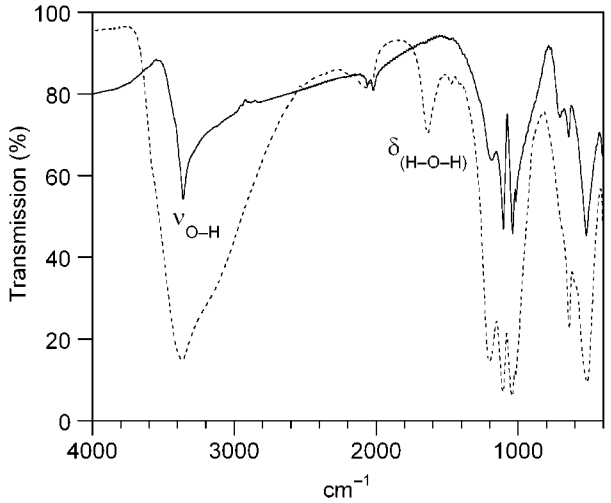

Figure 3. IR spectra of $NaV_3(OH)_6(SO_4)_2$ prepared by method 2 (solid line) and by a conventional nonredox precipitation (dashed line).

the presence of the H−O−H moiety within the intralayer and interlayer of the jarosite structure. The correlation between depressed transition temperatures and the presence of site defects in the Kagomé lattice appears to be a general trend for the jarosite compounds. Recent magnetic studies performed on stoichiometrically pure A^+ members of Fe^{3+} jarosites yielded reproducible antiferromagnetic ordering temperatures that were appreciably greater than those previously reported.[36] Our results

(36) Grohol, D.; Papoutsakis, D.; Nocera, D. G. Submitted for publication.

Table 3. Locations of Peaks in Infrared Spectra of the $AV_3(OH)_6(SO_4)_2$ Jarosites[a]

mode	NaVS	KVS	RbVS	TlVS	NH_4VS
ν(O−H)	3361	3386	3413	3412	3412
ν(N−H)	-	-	-	-	3286
δ(N−H)	-	-	-	-	1425
ν_{as}(S−O)	1188	1190	1200	1194	1196
ν_{as}(S−O)	1105	1095	1090	1078	1088
δ(V−O−H)	1040	1030	1018	1011	1016
δ_{as}(S−O)	706	702	688	merged	merged
δ_{as}(S−O)	644	642	667	658	671
ν(V−O)	521	521	515	503	513

[a] Assignments taken from refs 33 and 35.

may also be of relevance to the magnetic properties of jarosites possessing H_3O^+ ions as the A^+ cation. For V^{3+} jarosite, $(H_3O)V_3(OH)_6(SO_4)_2$, a $T_c = 21$ K has recently been observed.[37] A possibility exists that the low T_c for this sample, as compared to that observed for other A^+ members of this series,[24] is due to defects arising from protonation of the hydroxides bridging the vanadium centers. More generally, jarosites with wide ranges of x values in eq 5 have been described in the literature for M = Fe^{3+}.[9,10] The end member of this ion exchange, $(H_3O)Fe_3(OH)_6(SO_4)_2$, has extensively been investigated, and it has long been believed to be a spin-glass magnetic system.[9,10,17] A possible explanation of this spin glass behavior may be due to structural disorder arising from proton transfer from the interlayer hydronium ions to the bridging hydroxyl groups.

(37) Wills, A. S. *Phys. Rev. B* **2001**, *63*, 064430/1−064430/13.
(38) Gopalakrishnan, J. *Chem. Mater.* **1995**, *7*, 1265−1275.

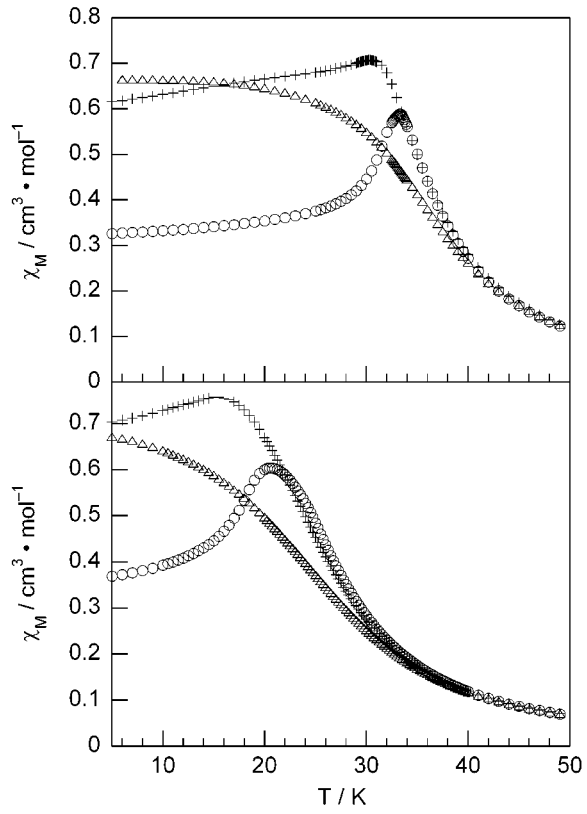

Figure 4. Temperature dependence of *M*/*H* per mole of vanadium at applied magnetic field strengths of 0.5 (○), 5.0 (+) and 10.0 (△) kOe for a sample prepared by (bottom) conventional nonredox- and (top) redox-based hydrothermal syntheses.

Concluding Remarks

Low-temperature synthetic techniques such as "chimie douce", flux, or solvothermal methods[38−40] permit control over the reaction pathway under mild conditions (T < 300 °C) as compared to traditional high-temperature solid-state synthetic protocols.[41−43] However, precipitation is often rapid when cations and anions, exhibiting high thermodynamic affinities to each other, are reacted under *homogeneous* conditions. If the nucleation rate of new crystals significantly exceeds the growth rate of crystals already formed[44] then microcrystalline powders will result that may or may not be stoichiometrically pure. Under extreme conditions, local deficiencies will be created when the precipitation rate is faster than ion diffusion. As is the case for jarosite materials, an available charged ion may substitute locally depleted ions to yield poorly crystalline products that contain a variety of structural and stoichiometric defects.

The newly discovered synthetic methods described herein are designed to generate the magnetic M^{3+} ion by controlled redox reactions under equilibrium. Under these hydrothermal conditions, highly pure materials can be obtained.

The idea of introducing a step to control the production of a metal ion prior to precipitation is not new, although previous solvothermal protocols have not typically involved a redox step. Rather, the metal ion was produced by its controlled dissolution from a heterogeneous phase. Alberti and co-workers synthesized large single crystals of α-zirconium phosphate by taking advantage of the temperature-dependent equilibrium between F^- and Zr^{4+} ions.[45] As the temperature was slowly raised, Zr^{4+} ions were de-complexed and made available for reaction with the phosphate anion. This method was subsequently employed for the preparation of organic derivatives of α-zirconium phosphate and phosphonates and for the synthesis of a variety of phosphonate compounds possessing transition metal cations other than Zr^{4+}. Zhang and Clearfield have used an alternative approach to grow single crystals of divalent transition metal phosphonates.[46] In aqueous environment, urea slowly decomposes to generate ammonium hydroxide, thereby gradually increasing the pH of the solution. In an environment with an increasing pH, phosphonic acids can be slowly deprotonated and thus made available for reaction with the transition metal to form divalent phosphonates.

In summary, we have prepared and structurally characterized a new series of vanadium jarosites. We have demonstrated that representatives of the jarosite class of materials can be obtained by deliberately inserting a kinetically controlling oxidation or reduction step into the synthesis sequence in such a way as to slow the formation of the product. With this approach, we have developed three new methods for the synthesis of vanadium jarosites in pure form and of high crystallinity. The described synthetic methods are general and should be applicable to other members of the alunite supergroup of minerals. For instance, ongoing investigations exploiting redox-based hydrothermal methods have yielded large and stoichiometrically pure single crystals of the Fe^{3+} jarosites. Our studies of the V^{3+} and other M^{3+} jarosites reveal that these new redox-based synthetic approaches are keystones to obtaining reproducible magnetic properties of the Kagomé lattice of the jarosite class of compounds.

Acknowledgment. We thank Dr. Dimitris Papoutsakis for acquiring the X-ray single crystal data sets. Financial support for this work was provided by the National Science Foundation (DMR-9311597) and by the Center for Materials Science and Engineering Research at MIT (DMR-9808941).

Supporting Information Available: Tables of crystal data, ORTEP representations with numbering schemes, atomic coordinates, and isotropic and anisotropic thermal parameters for $AV_3(OH)_6(SO_4)_2$ (A = Na^+, K^+, Rb^+ and Tl^+) (PDF). An X-ray crystallographic file in CIF format. This material is available free of charge via the Internet at http://pubs.acs.org.

JA016832U

(39) Stein, A.; Keller, S. W.; Mallouk, T. E. *Science* **1993**, *259*, 1558−1564.
(40) Rouxel, J.; Tournoux, M.; Brec, R. *Soft Chemistry Routes to New Materials*; Trans Tech Publications: Aedersmannsdorf, CH, 1994; Vol. 152−153.
(41) Corbett, J. D. *Inorg. Chem.* **2000**, *39*, 5178−5191.
(42) West, A. R. *Solid State Chemistry and Its Applications*; Wiley: New York, 1984.
(43) Hagenmuller, P. *Preparative Methods in Solid State Chemistry*; Academic Press: New York, 1972.
(44) Leubner, I. H. *J. Phys. Chem.* **1987**, *91*, 6069−6073.
(45) Alberti, G.; Costantino, U.; Giulietti, R. *J. Inor. Nucl. Chem.* **1980**, *42*, 1062−1063.
(46) Zhang, Y.; Clearfield, A. *Inorg. Chem.* **1992**, *31*, 2821−2826.